



Technical Note

The Detector Angular Offset & Instrument
Mode Mask Calibration Products

Ref: SPIRE-RAL-NOT-
003225

Issue: 1.1

Date: 2 July 2009

Page: 1 of 12

SPIRE Detector Angular Offset and Instrument Mode Mask Calibration Products

Edward Polehampton & Marc Ferlet

1.1 Reference Documents

RD1	Calibration Products for SPIRE Data Processing	SPIRE-RAL-DOC-002261
RD2	SPIRE Instrument User Manual, Issue 1.0	SPIRE-RAL-PRJ-002395
RD3	Definition of a combined focal plane aperture for the SPIRE instruments, Issue 1.0, 25 January 2001	SPIRE-RAL-NOT-000581
RD4	SPIRE Instrument PFM Filters End Item Data Package (EIDP)	SPIRE-UCF-DOC-002185
RD5	SPIRE Spacecraft-Instrument Alignment Matrix (SIAM)	SPIRE-RAL-NOT- 002881
RD6	SPIRE Pixel identification from optical model Excel spreadsheet, version 6	

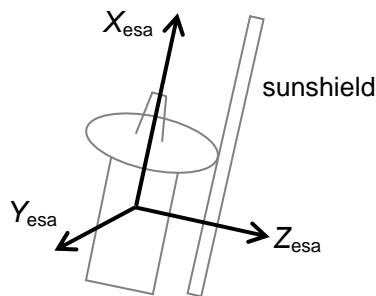
1.2 Introduction

These calibration products provide the angular offsets of the detectors in each array, and specify an integer mask that can be used to identify which detectors are chopped out of the field of view when the BSM is moved. The Instrument Mode Mask product is divided into separate tables for each "Instrument Mode" (ie. POF2, POF3) as the BSM chop throw will be different in each. This mask is used in the demodulation and denodding tasks to ensure that the final map given to astronomers does not include areas where the inside of the instrument has been combined with the sky. This document describes the background needed to determine the detector offsets and which detectors to include in the instrument mode mask calibration product for the Photometer, and to explain why a similar product is not required for the Spectrometer.

1.3 Locations of specific detectors in the field of view

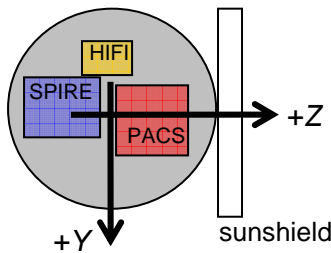
The positions of detectors in the field of view are determined from the spreadsheet, *SPIRE_Pixel_identification_from_optical_model_v6.xls* (RD6) – this is an extension of the *SPIRE Spacecraft-Instrument Alignment Matrix* (RD5) to cover all detectors. This spreadsheet gives the position of each detector in mm in the focal plane in the ESA system (X_{esa} , Y_{esa} , Z_{esa}), and the direction cosine vectors for each detector (A_{esa} , B_{esa} , C_{esa}). These direction cosine vectors are used in the SIAM to specify the direction cosine matrix that transforms the Herschel centred coordinate system to a system centred at any one of the SPIRE aperture positions.

The spacecraft X, Y and Z axes are specified as follows:

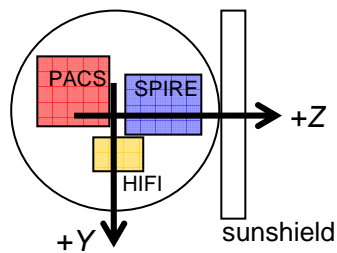


Several points that are important to note when interpreting the spreadsheet:

1. The X, Y, Z coordinate system is fixed with respect to the satellite
2. The optics of the telescope cause a flip-rotation about the X axis such that a movement on the instrument plane *towards* the sunshield (*positive Z*) causes a movement *away* from the sunshield on the sky (*negative Z*). The same effect also occurs in the Y-direction (*positive* movement in Y on the focal plane is *negative* movement in Y on the sky).



Instruments as seen on the focal plane from M2



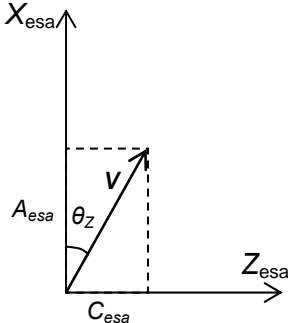
Herschel FOV on the sky with instrument positions

The angular positions of each SPIRE detector in the coordinate system centred at the Herschel boresight, along the spacecraft Y and Z axes are given by,

$$\theta_Y = \frac{\pi}{2} - \cos^{-1}(B_{esa})$$

$$\theta_Z = \frac{\pi}{2} - \cos^{-1}(C_{esa})$$

This correction is calculated as follows (example for just the Z component):



We are interested in the angular position in the Z direction – i.e. θ_Z

The direction cosine vector specifies the normalised vector in the direction of that detector ($\|\vec{V}\|=1$). Strictly this applies in 3D, but as the angles are small, we can make an approximation that is true in the 2D plane of each component*, and calculate the angular position using,

$$\theta_Z = \sin^{-1}\left(\frac{C_{esa}}{\|\vec{V}\|}\right) = \frac{\pi}{2} - \cos^{-1}\left(\frac{C_{esa}}{\|\vec{V}\|}\right)$$

In order to determine the angular offsets of the detectors *within* the SPIRE aperture coordinate system, we need to know their positions relative to the SPIRE aperture used,

$$\theta_{Y_{SPIRE}} = \theta_{Y_{det-Herschel}} - \theta_{Y_{aperture-Herschel}}$$

$$\theta_{Z_{SPIRE}} = \theta_{Z_{det-Herschel}} - \theta_{Z_{aperture-Herschel}}$$

The locations of detectors in the SPIRE S14 aperture coordinate system for each array are shown in Figure 1.

*Note: the strict calculation in 3D would be, $\theta_Z = \tan^{-1}\left(\frac{C_{esa}}{A_{esa}}\right)$

but the difference in angular position with the formula above is at most 0.002°.

1.3.1 Example to determine the position of PSWJ15 relative to aperture S14

From the spreadsheet, aperture S14 is centred at PSWE8.

On the instrument focal plane in millimetres:

Position of PSWE8: $Y_{esa} = -2\text{mm}$, $Z_{esa} = -90.6\text{mm}$

Position of PSWJ15: $Y_{esa} = -32.45\text{mm}$, $Z_{esa} = -105.74\text{mm}$

Therefore, the relative position of PSWJ15 on the instrument plane with respect to PSWE8 is, (-30.45mm, -15.14mm)

which is in the negative-negative quadrant of the Y-Z plane.

On the sky in arcseconds:

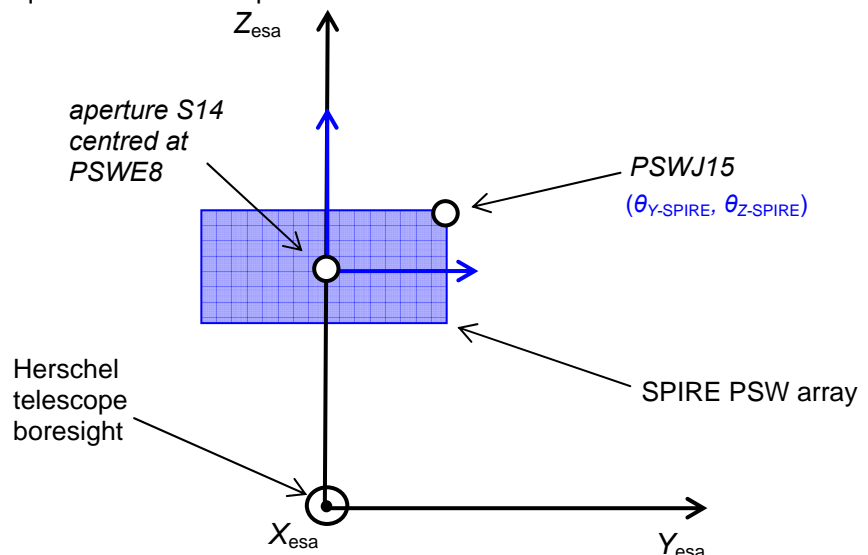
Direction cosine vector to PSWE8 = [0.999994000, 0.000243700, 0.003449100]

Direction cosine vector to PSWJ15 = [0.999991200, 0.001317460, 0.003972900]

Applying the equations above gives the relative angular offset of PSWJ15 with respect to PSWE8 as, (221.5", 108.0")

which is in the positive-positive quadrant of the Y-Z plane.

PSW location on the sky:



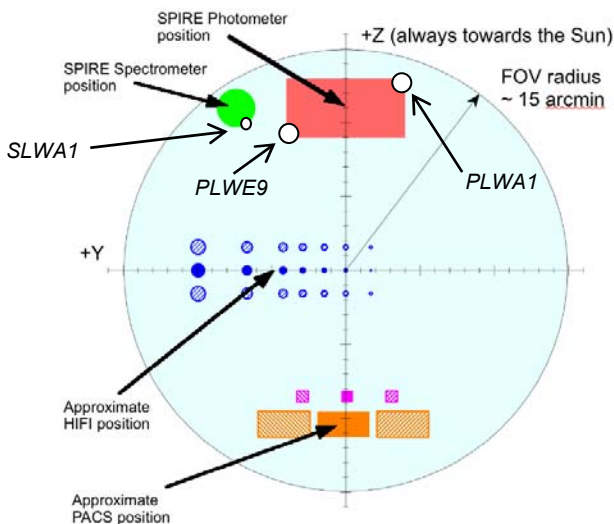
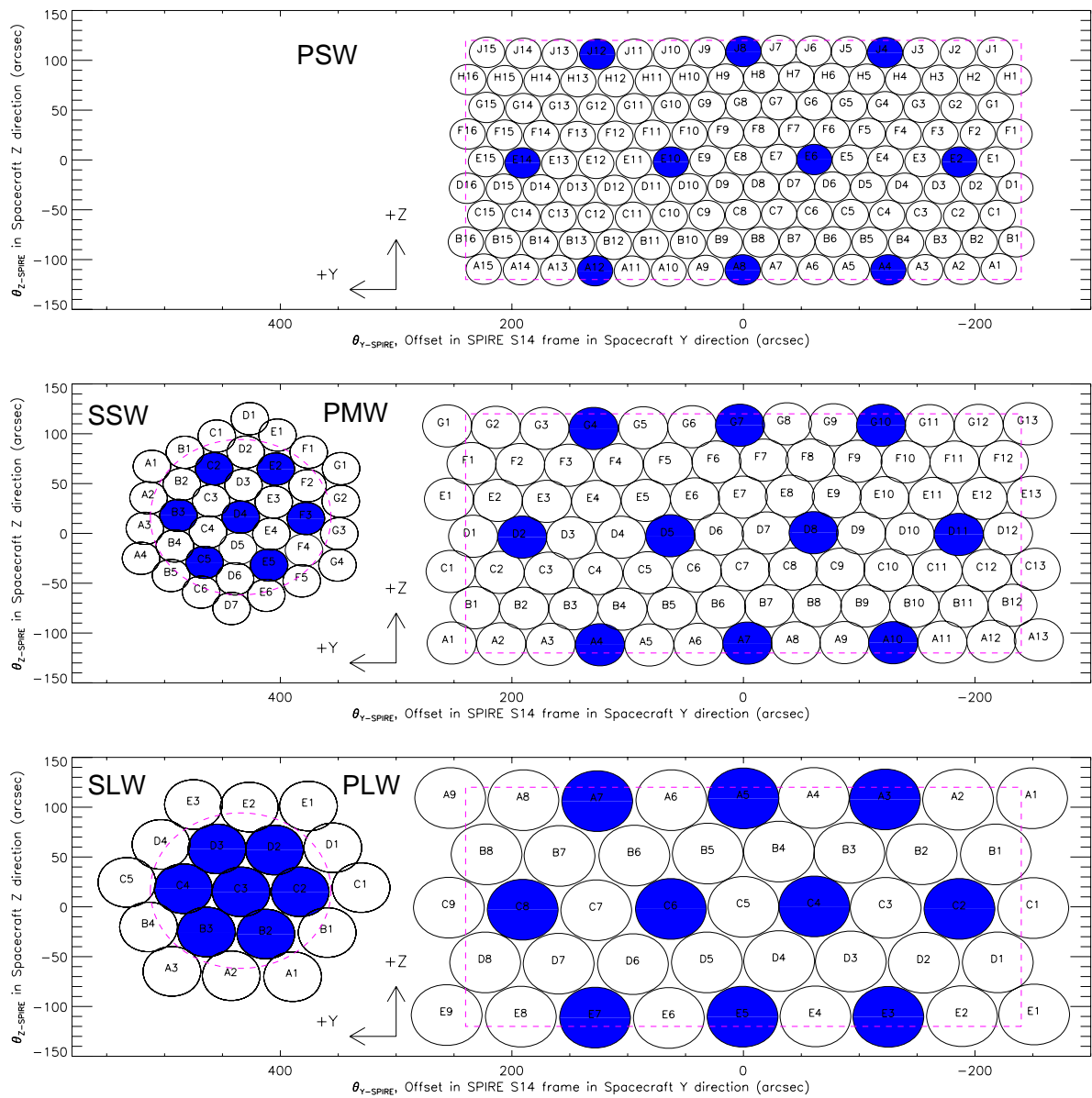


Figure 1: The location of specific detectors in the Spire frame centred at aperture S14 (upper plots). The coaligned detectors are coloured blue. The 8'x4' boundary is shown for the Photometer and the 2.6' field for the Spectrometer. The plot on the left shows the locations of the Photometer and Spectrometer in the frame centred at the Herschel boresight from HSpot, with the Sun direction marked. **All plots show the positions on the sky rather than in the instrument plane.**

1.4 Background to Instrument Mode Mask

An Instrument Mode Mask is required to take account of the effect of the limiting apertures within the instrument that restrict the field of view on the sky. There are several places in the optical train that limit the field of view on the detector arrays – the aperture at the Herschel focal surface, and the reflective surface of mirror M6 (PM6 for Photometer, and SM6 for Spectrometer). For the Spectrometer, there is an additional dynamic vignetting caused by a mismatch with SM12 which changes with SMEC position. This causes the OPD dependent vignetting which shows up as a droop in the baseline of the interferograms.

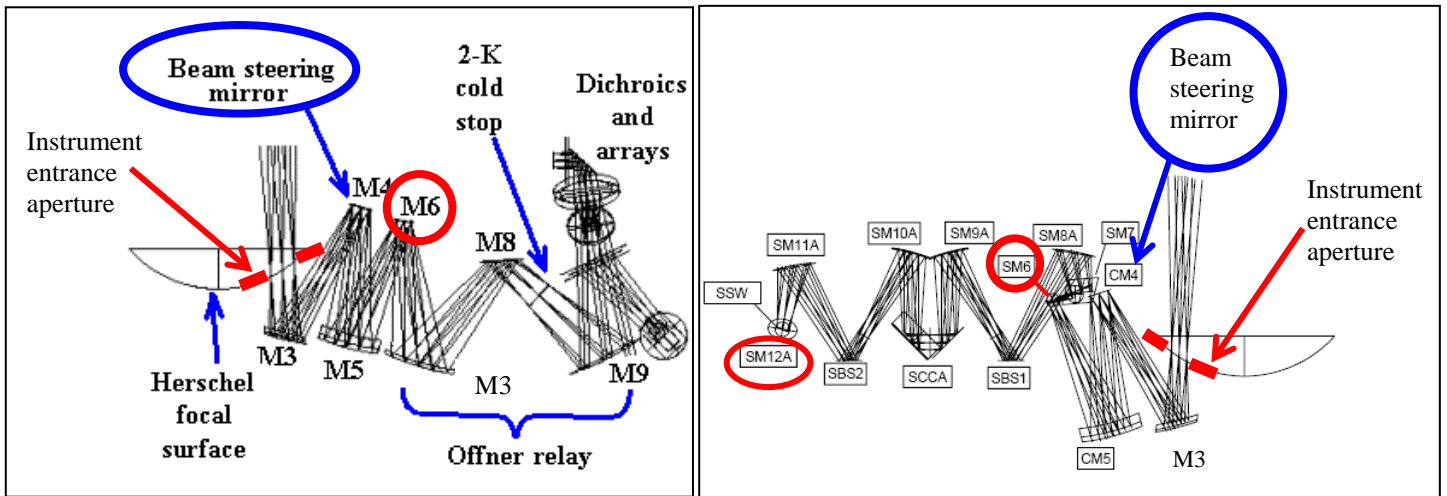


Figure 2: The Photometer (left) and Spectrometer (right) optical designs showing the instrument entrance aperture, beam steering mirror (M4), PM6, SM6 and SM12 (from the Instrument User Manual). Only the upper half of the spectrometer optics are shown.

In summary, the three effects are:

Cutoff due to entrance aperture	Changes with BSM position	Photometer & Spectrometer
Field effect (static) vignetting	Fixed with respect to detector positions	Photometer (PM6) & Spectrometer (SM6)
Pupil effect (dynamic) vignetting	Changes with SMEC position	Spectrometer (SM12)

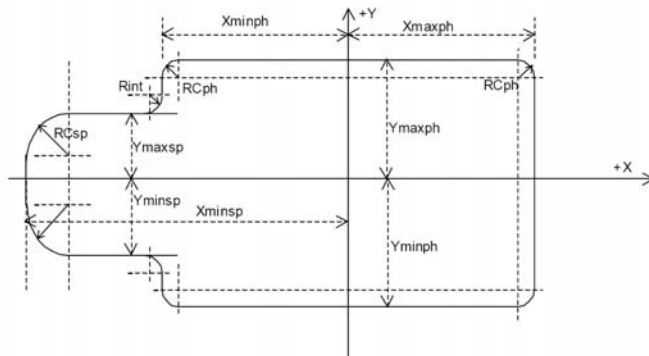
1.4.1 Entrance Aperture

As the entrance aperture is before the BSM in the optical train, the detector arrays are moved under this aperture as the BSM moves. Figure 3 shows a photograph of the aperture taken in the lab during PFM testing.

The specification for the entrance aperture is given in RD3 (Figure 4 and Table 7 of that document). The dimensions of the aperture are reproduced here in Figure 4 (from RD3) and 5 from (RD4).



Figure 3: Photograph of the instrument entrance aperture (during PFM testing).



Dimension Label in figure 4	Value (mm)
Xmaxph	39.316
Xminph	-52.088
Ymaxph	23.596
Yminph	-22.992
RCph	2.0
Rint	4.0
Xminsp	-77.108
Ymaxsp	16.407
Yminsp	-16.889
RCsp	10.0

Figure 4: The dimensions of the entrance aperture from RD3.

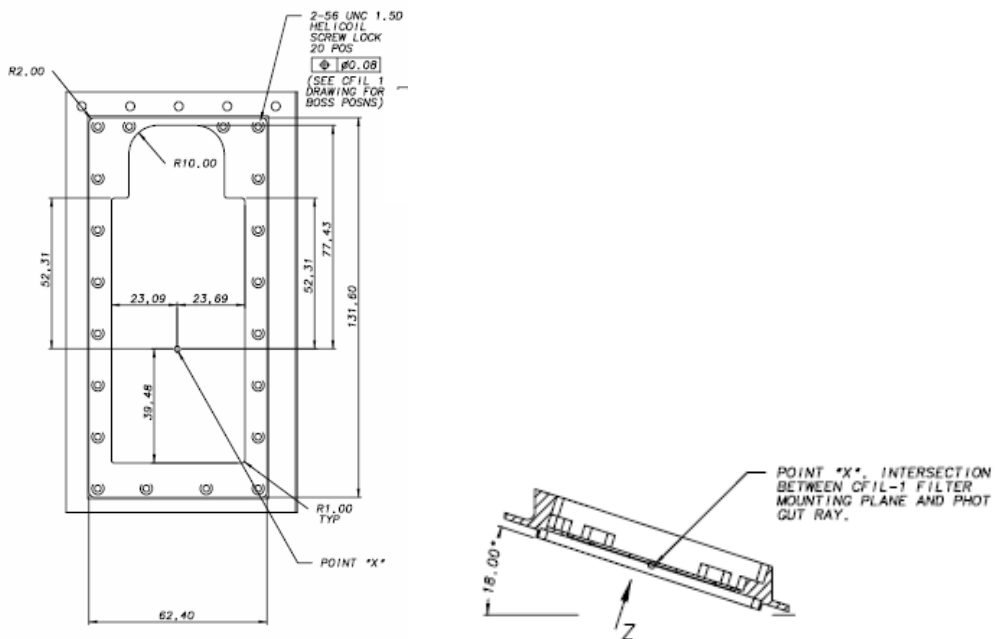


Figure 5: The dimensions of the entrance aperture from RD4.

The entrance aperture is located at the Herschel focal surface and so is tilted at 18° in order to match the focal surface curvature. As the aperture is not curved itself, only the central axis is actually on the focal surface and this means that the shape should be slightly distorted when projected onto the sky. However, assuming this distortion is negligible, the size of the aperture on sky can be determined from the plate scale. Measured data for the telescope indicate a flight value for the focal length of 28.623m. SPIRE is offset in the telescope focal plane (actually curved) and so the effective focal length is slightly reduced, giving a plate scale of around $7.28''/\text{mm}$. This should only vary at % or sub % relative level across the SPIRE field of view. The resulting aperture with the positions of the detectors is shown in Figure 6. As the dimensions of the aperture in RD3 and RD4 agree to within 0.5 mm, the (slightly smaller) values from RD3 have been used here. The (0,0) position is set to PSWE8 – this corresponds to point "X" in Figure 4, which is defined from Herschel Optical Datum to be $x=233.9097$ mm, $y=0.00$ mm and $z=-90.3532$ mm in RD4. The separation between PSWE8 and SSWD4 is $(-434.27'', -16.25'')$, determined from RD5. The reason that the centre of the Spectrometer array is offset in both Y and Z directions is that the Herschel focal plane is curved in both directions, but the aperture is flat and the 18° tilt only allows for the curvature in the Z-direction.

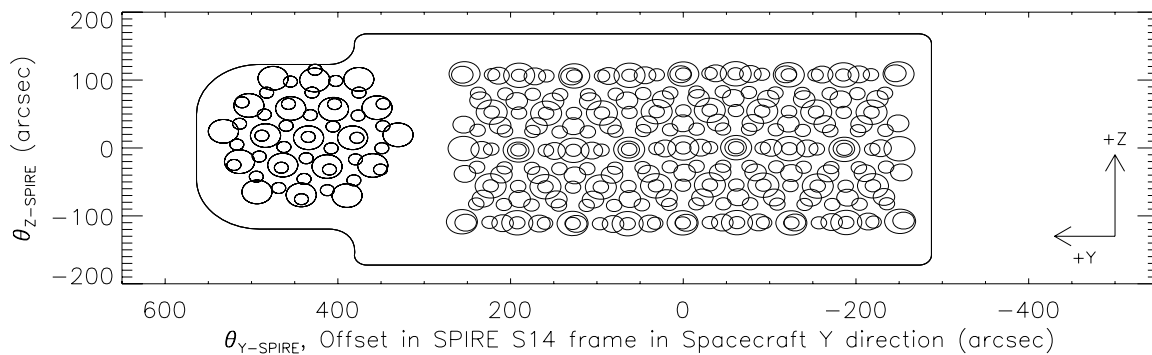


Figure 6: The location of the Photometer and Spectrometer arrays within the entrance aperture in spacecraft Y-Z coordinates on sky (with PSW E8 as the origin). Figure 1 gives the mapping between position and detector name for all arrays.

1.4.2 Field Effect Vignetting

The mirrors PM6 and SM6 occur in the optical train between the BSM and the detectors. They are oversized with respect to the beam centres of individual detectors, but not with respect to the full beam sizes, and this means that they cause a static vignetting to the outer detectors in the array.

For the Photometer, the oversizing of the mirror is correct for PSW, but with the larger beam sizes of PLW, there is some vignetting of the outer detectors. This has been observed in the lab data. For the spectrometer, there is vignetting of the outer ring of detectors. Figure 8 shows the mirrors PM6 and SM6 with the positions of the detector centres marked for PLW and SSW. The coloured dots correspond to a point source observed with each detector – i.e. the mirrors are not exactly at an image plane, so a point source appears extended (by a differing amount across the mirror). This shows that although the beam *centres* all fall within the boundaries of the mirror, part of the *full beam footprint* can fall off the edge, particularly for the spectrometer (the coloured ellipses represent a *single point* at beam centre – they do not show the whole beam size, which will be much bigger).

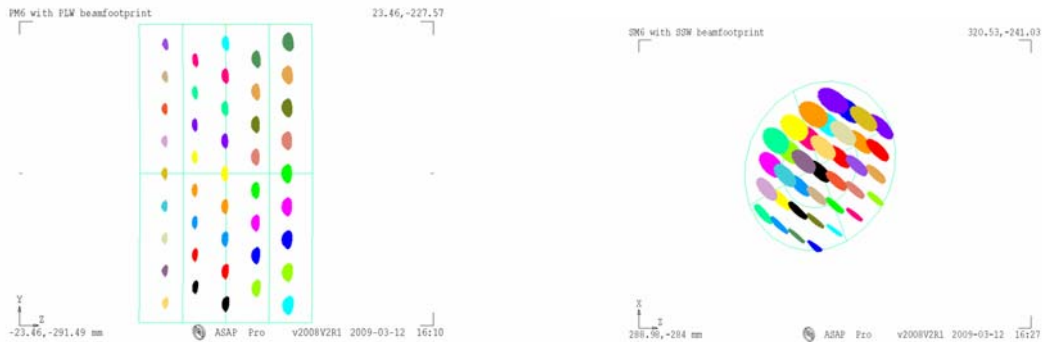


Figure 8: The position of detector *centres* on mirrors PM6 (for PLW) and SM6 (for SSW). Note that each coloured ellipse represents a single point and not the full beam footprint.

These mirrors are the origin of the quoted unvignetted fields of view in the descriptions of the instrument. These are usually quoted as 8'x4' for the Photometer and a circle of diameter 2.6' for the Spectrometer. In actual fact, these are just approximations to show the boundary inside of which all of the flux should be recovered. The actual transmission across the arrays has been measured in the lab and is not symmetrical.

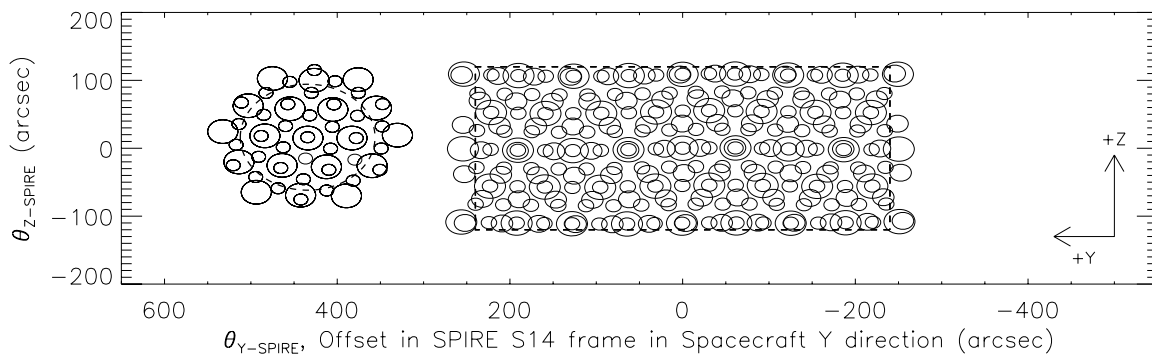


Figure 9: Detectors with nominal boundaries of static vignetting.

1.4.3 Pupil Effect Vignetting

There is a further vignetting for the Spectrometer that depends on the optical path difference. This is due to the fact that the beam changes size depending on the position of the SMEC. The mirror SM12 is located between the SMEC and the detectors, and is not oversized sufficiently to reflect all of the beam at all SMEC positions. This causes a fall off in transmission for the off-axis detectors that is dependent on SMEC position. Figure 10 shows the effect on the interferograms for SSW, with a fall off in transmission towards higher OPD (the central detector does not show this dynamic OPD-dependent vignetting because the full flux is always reflected by the mirror at all SMEC positions).

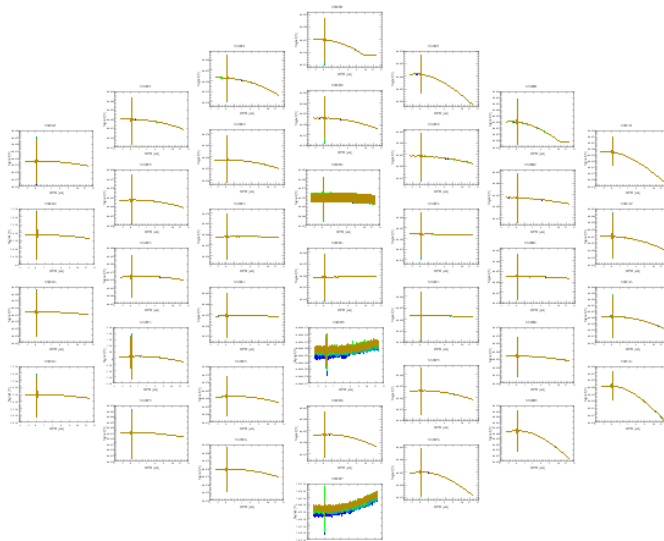


Figure 10: Interferograms for all detectors in the SSW array showing the dynamic vignetting which increases for detectors away from the axis.

1.5 Photometer Chopped Observations

In Photometer chopped observations, the BSM moves the detector array footprint on the sky underneath the entrance aperture. During this chopping, some detectors at the edge of the array may end up outside of the boundary of the aperture, and so only receive radiation from the (cold) inside of the instrument.

Or from the alternative point of view, the BSM moves the sky and entrance aperture over the detector array. If the chop throw is large enough, the edge of the aperture may be moved into the edge of the array, meaning those detectors only receive radiation from the inside of the instrument.

The current chop throws are as follows:

	Chop Throw	Jiggle Positions
POF2	63"	7
POF3	126"	64

For POF2 observations, the jiggle offsets are relatively small and we can just mask detectors which have any part of their beam footprint outside of the aperture. However, for POF3, the jiggle pattern is larger, and so some detectors may be inside for some jiggle positions and outside for others.

The simplest solution would be to mask all detectors which have *any* jiggle position outside of the aperture.

Figure 11 shows the detectors chopped outside the field for POF2 (individual jiggle positions not shown). In Figure 12, all jiggle positions are plotted (with beam sizes 18", 25", and 36"), showing the masked detectors (in blue). In these figures, detectors that should be masked on the right hand side of the aperture are coloured in blue. In Figure 12 it is also clear the two detectors must also be masked on the left hand side for PMW and PLW.

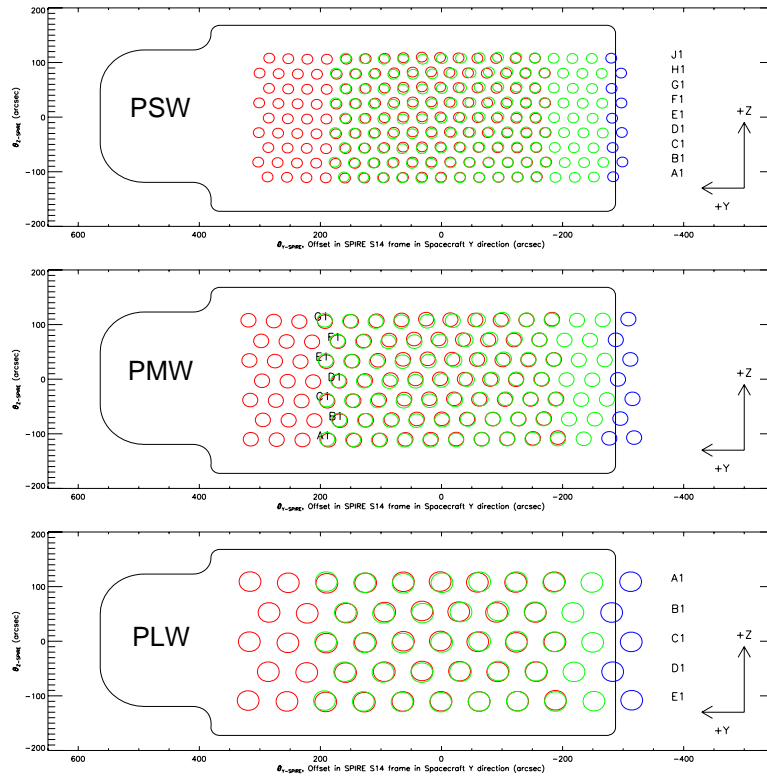


Figure 11: Detector positions in the aperture for POF2 with a chop throw of 63". The left chop is shown in red, and the right chop in green. Masked detectors are shown in blue.

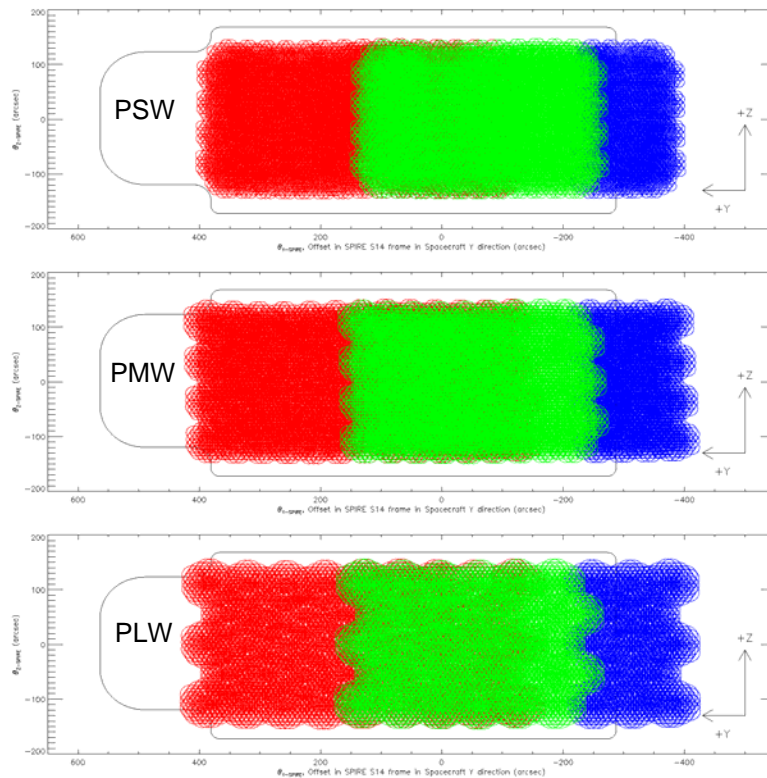


Figure 12: Detector positions for a POF3 64 point jiggle observation with a chop throw of 126". The left chop is shown in red, and the right chop in green. Masked positions are shown in blue.



Technical Note

The Detector Angular Offset & Instrument Mode Mask Calibration Products

Ref: SPIRE-RAL-NOT-003225

Issue: 1.1

Date: 2 July 2009

Page: 11 of 12

The final masked detectors should be:

POF2

- o PSWA1, PSWB1, PSWC1, PSDW1, PSWE1, PSWF1, PSWG1, PSWH1, PSWJ1
- o PMWA12, PMWA13, PMWB12, PMWC13, PMWD12, PMWE13, PMWF12, PMWG13
- o PLWA1, PLWB1, PLWC1, PLWD1, PLWE1

POF3

- o PSWA1, PSWA2, PSWA3, PSWB1, PSWB2, PSWB3, PSWC1, PSWC2, PSWC3, PSDW1, PSDW2, PSDW3, PSWE1, PSWE2, PSWE3, PSWF1, PSWF2, PSWF3, PSWG1, PSWG2, PSWG3, PSWH1, PSWH2, PSWH3, PSWJ1, PSWJ2, PSWJ3, PSWB4, PSDW4, PSWF4, PSWH4, PSWA4, PSWC4, PSWE4, PSWG4, PSWJ4
- o PMWA11, PMWA12, PMWA13, PMWB10, PMWB11, PMWB12, PMWC11, PMWC12, PMWC13, PMWD11, PMWD12, PMWE11, PMWE12, PMWE13, PMWF11, PMWF12, PMWG11, PMWG12, PMWG13, PMWD1
- o PLWA1, PLWA2, PLWB1, PLWB2, PLWC1, PLWC2, PLWD1, PLWD2, PLWE1, PLWE2, PLWC3, PLWE3, PLWA3

In addition, the following detectors should be masked on the left hand side of the aperture for POF3

- o PMWA1, PMWG1
- o PLWE9, PLWA9

An alternative solution would be to store the entrance aperture boundary in a calibration file, and mask specific jiggle positions in a new module in the code. The advantage of this method would be that only the actual pointings outside of the aperture would be masked, and also it would not matter if the chop throw or jiggle pattern was changed later.

1.6 Spectrometer Jiggled Observations

The Spectrometer does not have chopped observations, but does make jiggled maps:

	Chop Throw	Jiggle Positions
SOF2 int	0"	4
SOF2 full	0"	16

The jiggle positions are plotted over the aperture in Figure 13 (with beam sizes of 16.3" for SSW and 35" for SLW). This shows that some detectors (or positions) may need to be masked out in the spectral cube creation stage.

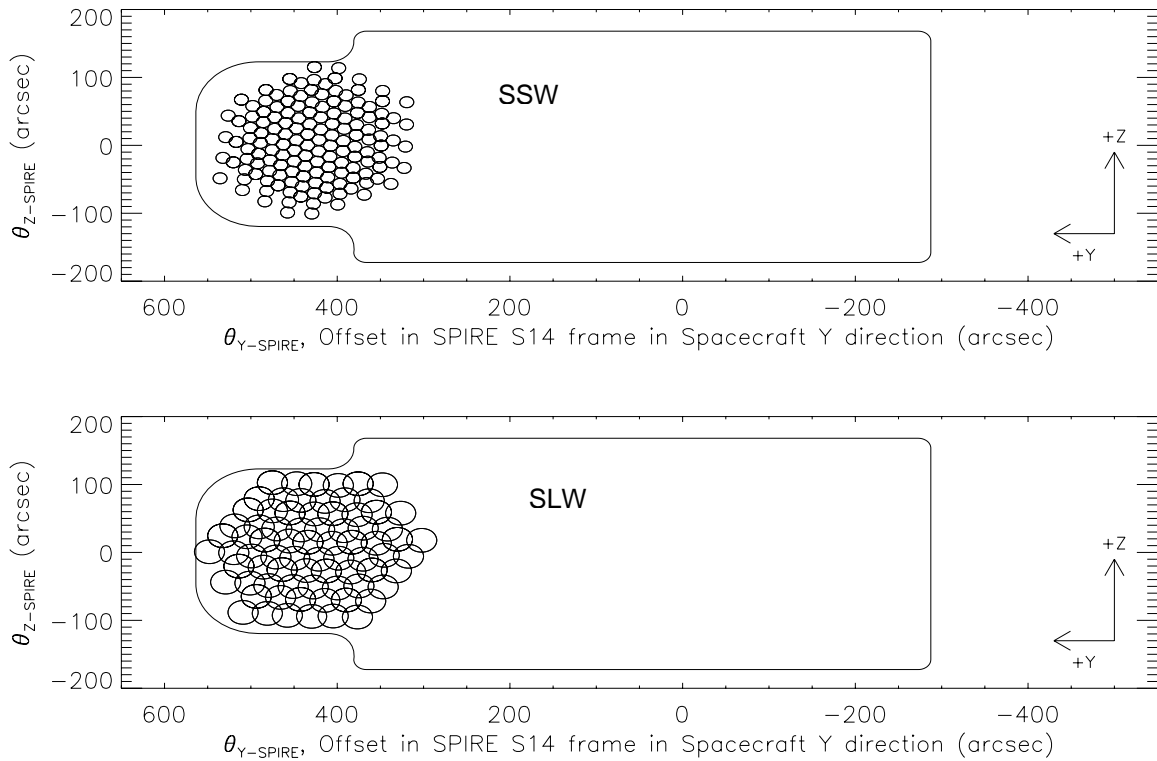


Figure 13a: Positions in a Spectrometer intermediate sampled Jiggle map over the aperture.

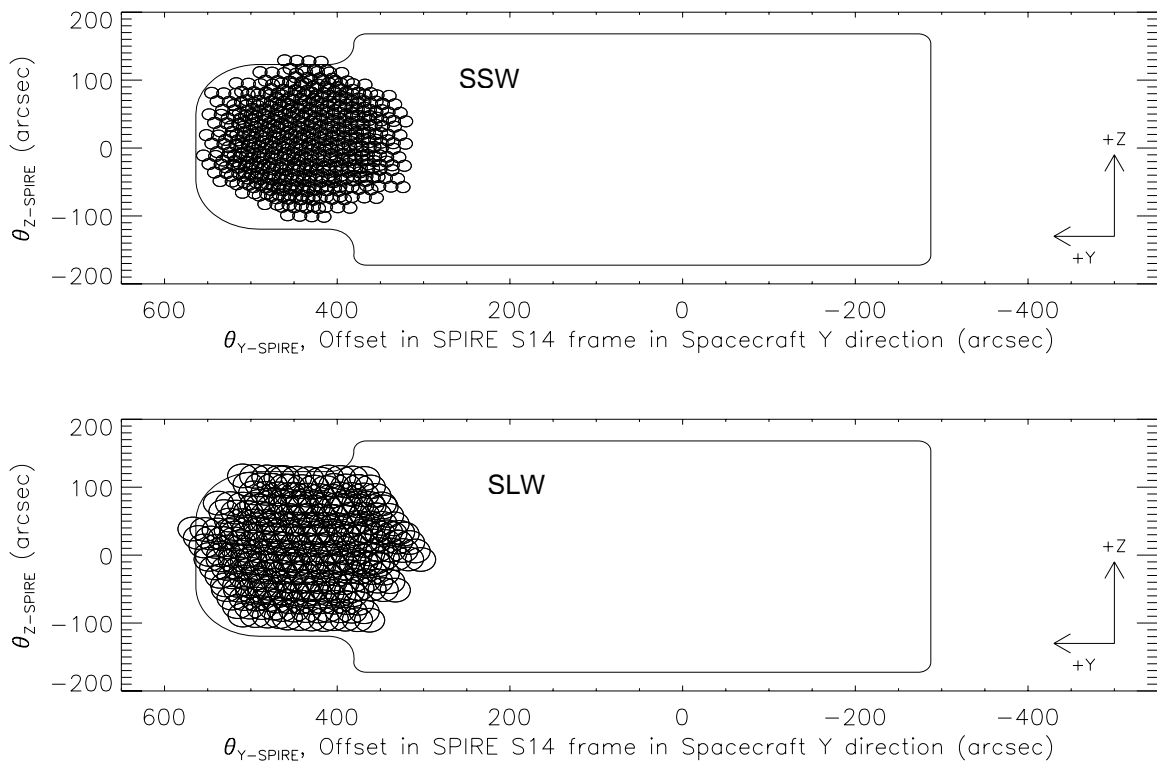


Figure 13b: Positions in a Spectrometer fully sampled Jiggle map over the aperture.